

## A region growing algorithm for robust kt-points B1+ homogenisation at 9.4T

Michael Stephen Poole<sup>1</sup>, Desmond H Y Tse<sup>1</sup>, Kaveh Vahedipour<sup>1</sup>, and N Jon Shah<sup>1,2</sup>

<sup>1</sup>INM-4, Forschungszentrum Jülich, Jülich, Germany, <sup>2</sup>Department of Neurology, RWTH Aachen University, Aachen, Germany

### Target Audience

Researchers that require uniform excitation at 7 T and above.

### Purpose

B1+ homogenisation was performed at 9.4 T repeatably and robustly using a region-growing algorithm. Radiofrequency pulse amplitudes and phases for kt-points homogeneous excitation<sup>1</sup> can be found with deterministic or stochastic optimisation algorithms, which regularly yield suboptimal local or unrepeatable solutions. One approach is to perform many local optimisations with randomised initial guesses, however we hypothesise that there exists a smooth continuum from the small region solution (essentially transmitter phase coherence in the centre) to the globally optimum solution for the full homogenisation volume.

### Methods

Experiments were performed with a 9.4 T whole-body MRI system (Magnetom 9.4T, Siemens, Erlangen) with 8 channels of parallel RF transmit and receive. Mapping the B1+ of each channel was performed with the dual refocusing echo acquisition mode (DREAM) sequence<sup>2</sup> by 16 measurements with unique incremental phase rotations for each channel<sup>3</sup> and the following parameters: 17 slices, T2\* compensated timings,  $TE_{STE} = 2.22$  ms,  $TE_{FID} = 4.44$  ms, 7° degree nominal flip angle (FA) and 4 x 4 x 4 mm<sup>3</sup> voxel size.

kt-points homogenisation RF pulses were optimised using Matlab (The Mathworks, Natick, MA) and a magnitude least squares (MLS)<sup>4</sup> variable exchange algorithm with phase following and Tikhonov regularisation. A target homogenisation region was defined and ( $N_r$ -1) more regions were defined to have dimensions of  $n/N_r$  times the target region, integer  $n = 1$  to  $N_r$ . Repeatedly eroded masks could also be used.

A 160 mm diameter spherical water phantom containing 50 mM phosphate buffered saline, a formalin-fixed *ex vivo* human brain and a 41-year old healthy male volunteer (fully complying by the rules of the local ethics committee) were imaged using a low flip angle gradient echo (GE) sequence and kt-points homogenisation. Flip angle calibrations were performed by additional GE and actual flip angle imaging (AFI) scans with transmitter phases that represented the 1<sup>st</sup>, 2<sup>nd</sup> and 3<sup>rd</sup> principle component (PC) modes. These modes were calculated via singular value decomposition of the complex B1+ maps and normalised, to produce modes with complimentary interference patterns.

### Results

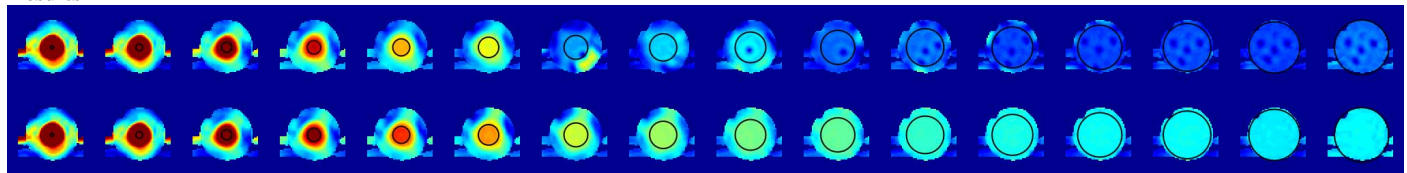


Figure 1. Illustrating the region-growing algorithm. Predicted relative FA (arbitrary units) in the mid-axial slice with 8 kt-points and B1+ maps measured using DREAM. Top row shows results from homogenising cylindrical regions, 30 mm thick, of increasing diameter (every 10 mm from 10 mm to 160 mm) without region growing. Bottom row shows the same with region growing - i.e. the starting point for MLS minimisation is the solution of the smaller region.

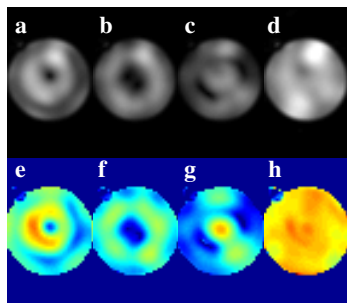


Figure 2. Calibrating the kt-points FA. FLASH data of PC modes 1-3, **a-c**, AFI data of PC modes 1-3, **e-g**, FLASH data with kt-points using region-growing (predicted bottom right Fig. 1), **d**, and the derived relative FA map, **h**.

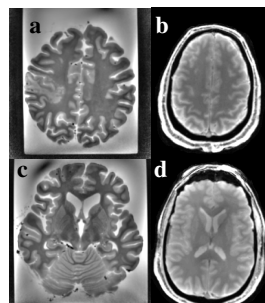


Figure 3. Two transverse slices of ex vivo, **a** & **c**, and in vivo, **b** & **d**, 3D FLASH data. The receive sensitivity weighting was removed by masked division by a Gaussian filtered image (filter width of 10 pixels).

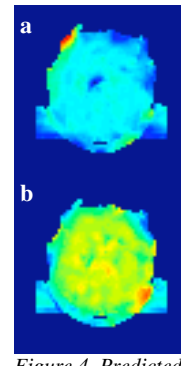


Figure 4. Predicted kt-points FA without, **a**, and with, **b**, region-growing in a failing example.

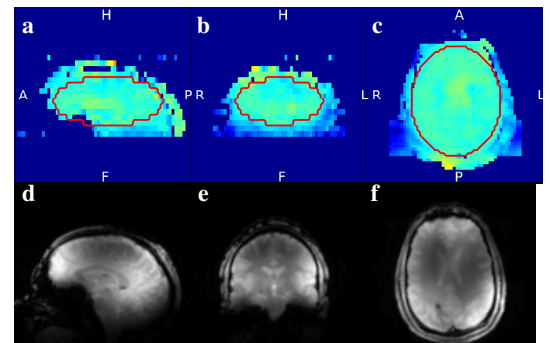


Figure 5. In vivo kt-points with 6 points and k-space positions at 6 m<sup>-1</sup>. Predicted FA maps (arbitrary units) in coronal, **a**, sagittal, **b**, and transverse, **c**, mid slices and GE data of the same slices, **d-f**, with TE = 3.9 ms, TR = 200 ms, 2 mm x 2 mm in-plane resolution and 3 mm slice thickness.

### Discussion

Due to the shortened RF wavelength at 9.4 T, holes appear in images because of destructive B1+ interferences. In the homogenisation of B1+ using kt-points, a deterministic algorithm is often used that find suboptimal local minima that is more troublesome in phantoms and also some human heads. This problem was avoided by using a region-growing algorithm. Figures 1 and 4 demonstrate the benefit of the region growing in a phantom and a troublesome head. Flip angle calibration<sup>1</sup> is shown in Fig. 2 in arbitrary units valid only for small tip angles, but extension to high tip angle is expected. This technique has also usefully been applied to "no holes" ( $\min\{1/\min(B1+)\}$ ) static B1+ shimming and is expected to benefit spokes excitations for slice-selective 2D imaging.

### Conclusion

Growing the region in kt-points results in repeatable and robust MLS optimised homogeneous excitation. It is not proven that this solution is globally optimal, but no superior solutions were found with randomised MLS or GA optimisations.

### References

<sup>1</sup>M A Cloos et al., *MRM* (2012) **67** p72, <sup>2</sup>K Nehrke and P Börnert, *MRM* (2012) **68** p1517, <sup>3</sup>D Tse et al., submitted to *ISMRM* (2014), <sup>4</sup>K Setsompop et al., *MRM* (2008) **59** p908.